

Influence of the C0 magnet multipole errors on the single beam dynamics in the Tevatron

Béla Erdélyi

This short note summarizes our systematic procedure to extract the multipole errors from the magnet measurements of the C0 dipoles (Lambertson and Cmag), and their effect on the single beam dynamics in the Tevatron (no beam-beam interactions included) when employed in tracking with MAD.

1 The fitting procedure

The magnetic field measurements have been provided by Hank Glass. The measurements were done with a 2-wire stretched wire system and supplied the integrated (over the length of the magnets) values of the vertical component of the magnetic field as a function of horizontal displacement from the magnet's center (x). The measurements were repeated on several planes parallel with the horizontal plane ($y = \text{constant}$), and at injection (500 A) and collision (4500 A) excitations.

We took a systematic approach in the fitting of the data to multipole strengths, with the hope that future fits of similar data will benefit from these studies. Several aspects of the fitting procedure have been studied. Recall that B_y must be an even function of y if all skew multipoles vanish. Since two sets of measurements were taken at $y = -0.375$ in and at $y = +0.375$ in respectively, it was possible to infer the existence of skew multipoles by mere inspection of the measurements. However, for the set of measurements belonging to the plane $y = 0$ only the normal components survive. Therefore, we studied whether it is more advantageous to extract the normal and skew multipoles separately. After trying many possible combinations of data sets and extraction methods, we concluded that the best way is to extract all multipoles simultaneously using every possible data point from all planes measured. Most likely this is due to the reduction of the statistical noise.

Another aspect studied was the objective function to be minimized. We found that the best results were obtained when the objective function was the total distance between the data points and the curves which are the graphs of the fitted magnetic fields.

Lastly, and perhaps most importantly, we tried several optimizers. Among the routines tried were the fitting capabilities of Mathematica (two kinds), and four implemented in the code COSY Infinity (simplex, parabolic minimizer, simulated annealing, and the Levenberg-Marquardt algorithm (LMDIF)). After extensive searches we obtained that the following procedure gives the smallest objective function in every case studied (and, of course, the best solution under visual inspection): starting with zero initial conditions for all multipoles LMDIF is used until the objective function does not change anymore. The final values produced by LMDIF are utilized as initial conditions for the simplex. Moreover, the simplex is wrapped into a loop in which the final values of a run are used as initial values for the next run. The loop is ended when the objective function does not change anymore. Sometimes the loop took as much as 500 iterations, since it is known that often the simplex stops at local minima. In summary, the LMDIF was the best in finding good initial conditions, and the simplex was the best in refining them.

Finally, we note that the fitting was carried out to sufficiently high orders, so that convergence was obtained (stability of the fitting procedure with respect to the fitting order was one criteria in the evaluation of the different methods). We also mention that the fitted

fields were enforced to satisfy Maxwell's equations at every fitting step. However, even if there is a nonzero skew dipole component, the measurements do not allow its determination, since its contribution vanishes from B_y at any point (x, y) .

1.1 The extracted multipole strengths

Here we present eight sets of multipoles: normal and skew multipoles at injection and collision for Lambertsons and C-magnets. For ease of implementing in tracking, the data is shown in the format compatible with the MAD MULTIPOLE element (the nomenclature should be obvious).

```
LAMB_NORM_INJ:    MULTIPOLE,&
    K1L = .000094676928803663, K2L = -.0013992607355682,&
    K3L = -.24159622525681165, K4L = -19.70497392363100,&
    K5L = 3055.82339748350570, K6L = 1223645.0598763579

LAMB_SKEW_INJ:    MULTIPOLE,&
    K1L = .77399428399893E-5, T1, K2L = .00632330671932732, T2,&
    K3L = .24793282901111363, T3, K4L = .22508463851924521, T4,&
    K5L = -4713.188144735338, T5, K6L = -429074.9245233797, T6

CMAG_NORM_INJ:    MULTIPOLE,&
    K1L = -.63279795733008E-5, K2L = .004592971981063561,&
    K3L = .004546445147202854, K4L = -146.42441098295123,&
    K5L = -13012.225072349556, K6L = -9829034.4923126064

CMAG_SKEW_INJ:    MULTIPOLE,&
    K1L = -.0000127455683259, T1, K2L = .00001250165727948, T2,&
    K3L = .90013108245498452, T3, K4L = 86.517606763314973, T4,&
    K5L = .2348940895066E-15, T5, K6L = 5920791.8499715198, T6

LAMB_NORM_COL:    MULTIPOLE,&
    K1L = .000122524723330439, K2L = .00170236439901443,&
    K3L = -.20367305734506921, K4L = .62702793475545682,&
    K5L = -256.60455434069831, K6L = -126146.1130949865,&
    K7L = 39524085.429174379

LAMB_SKEW_COL:    MULTIPOLE,&
    K1L = .379877189171711E-05, T1, K2L = -.0021575503170753, T2,&
    K3L = -.085767476119968725, T3, K4L = -.9383585224011014, T4,&
    K5L = -.42418416193744E-10, T5, K6L = 101583.93314579176, T6,&
    K7L = -10650332.1284534070, T7

CMAG_NORM_COL:    MULTIPOLE,&
    K1L = .00009128834363786, K2L = -.0049791416393087,&
    K3L = -2.640016243899867, K4L = 332.49173595941227,&
    K5L = 48536.076827766701, K6L = -32659799.01195792

CMAG_SKEW_COL:    MULTIPOLE,&
    K1L = .00001941615768780, T1, K2L = .01132567097298473, T2,&
    K3L = -.8319903017077779, T3, K4L = -361.6223384143220, T4,&
    K5L = 123928.62269710112, T5, K6L = 3345471.3522365289, T6
```

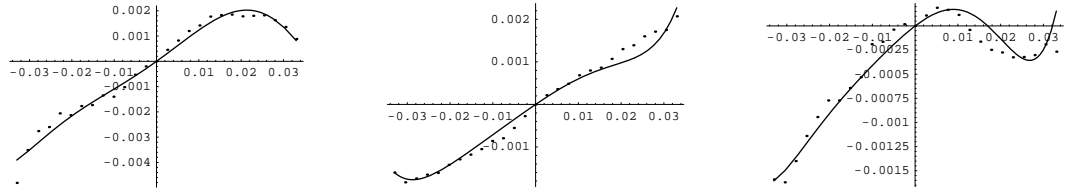


Figure 1: The curves represent the integrated vertical component of the magnetic field of the Lambertsons at injection fitted to the experimental data shown as dots. The figures correspond to the different planes: a) $y = -0.375\text{in}$, b) $y = 0$, and c) $y = +0.375\text{in}$.

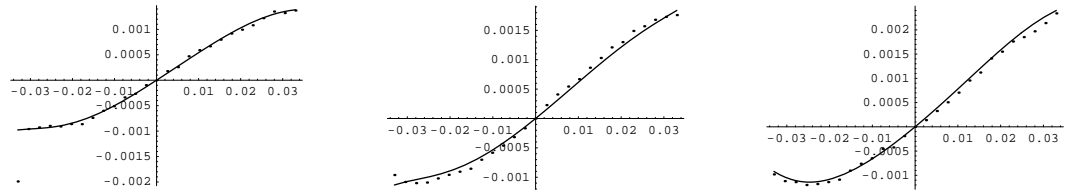


Figure 2: The curves represent the integrated vertical component of the magnetic field of the Lambertsons at collision fitted to the experimental data shown as dots. The figures correspond to the different planes: a) $y = -0.375\text{in}$, b) $y = 0$, and c) $y = +0.375\text{in}$.



Figure 3: The curves represent the integrated vertical component of the magnetic field of the C-magnets at injection fitted to the experimental data shown as dots. The figures correspond to the different planes: a) $y = 0$ and b) $y = +0.4\text{in}$.

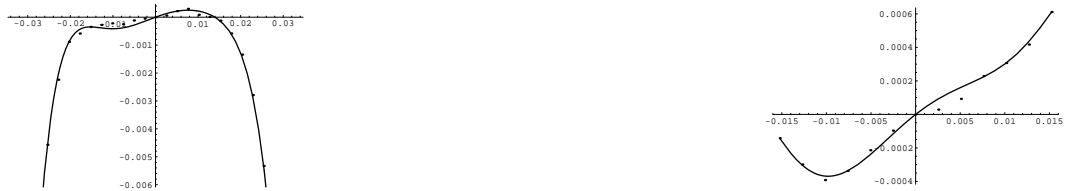


Figure 4: The curves represent the integrated vertical component of the magnetic field of the C-magnets at collision fitted to the experimental data shown as dots. The figures correspond to the different planes: a) $y = 0$ and b) $y = +0.4\text{in}$.

Energy	$\Delta\nu_x \cdot 10^3$	$\Delta\nu_y \cdot 10^3$
Injection	+1.1	-1.5
Collision	+2.7	-3.3

Table 1: Bare tune shift at injection and collision energies induced by the C0 magnet multipole errors.

Energy	$\langle \text{DA} \rangle$		DA_{\min}	
	C0 err. OFF	C0 err. ON	C0 err. OFF	C0 err. ON
Injection	9.5	9.4	8.0	7.0
Collision	13.2	13.0	12.0	11.0

Table 2: Dynamic aperture results of the studied cases. The minimum DA with errors drops by 1σ , while the average DA stays within 0.2σ .

The higher order coefficients vanish. Even most of the decapole and duodecapole coefficients are practically zero, since the fitting is over ± 1.3 inches at most. The fields, that correspond to these multipoles, and their comparison with measured data are shown in Figures 1 through 4, as a function of x .

2 Dynamics studies

Using the information presented in the previous section, the errors were implemented in MAD as thin multipoles in the middle of the corresponding dipoles. We investigated tune shifts, tune footprints, and dynamic apertures.

The bare tunes are shifted by the amounts shown in Table 1. Notice that overall the shifts are not large, and at collision they are more than twice larger than at injection. Inspection of the tune footprints in Figure 5 reveals that the size and shape of the footprints remain virtually unaltered. Finally, tracking gives the dynamic aperture shown in Table 2. Again, the average DA is essentially the same with and without errors, while, noticeably, the minimum DA drops by 1σ with the errors included. We note that the tunes were refitted to nominal values using quadrupoles in such a way to minimize linear optics changes.

In summary, the studies show that most likely the nonlinearities of the C0 Lambertsons and C-magnets do not harm the dynamics in any significant way.

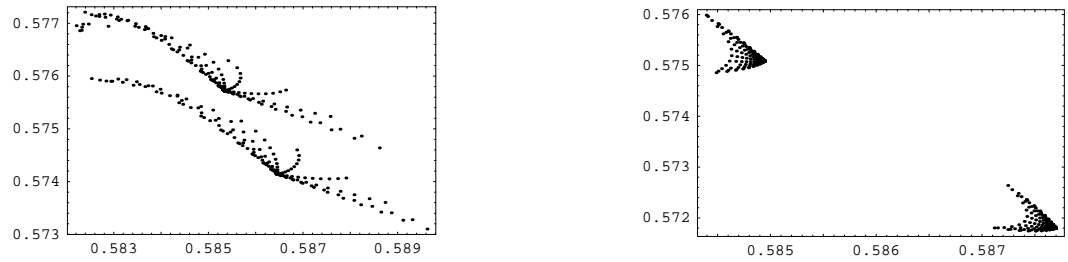


Figure 5: Tune footprints at *a*) injection and *b*) collision energies with C0 magnet multipole errors included, superimposed on the footprints without the errors.